Anharmonic effects and the two-particle continuum in the Raman spectra of $YBa_2Cu_3O_{6.9}$, $TlBa_2CaCu_2O_7$, and $Tl_2Ba_2CaCu_2O_8$

D. Mihailovic
Jozef Stefan Institute, University of Ljubljana, Jamova 39, Ljubljana, Slovenia

K. F. McCarty and D. S. Ginley
Sandia National Laboratories, Livermore, California 94551-0969 and Albuquerque, New Mexico 87185
(Received 22 July 1992, revised manuscript received 29 October 1992)

Anharmonic interactions of the apex O vibrations in $YBa_2Cu_3O_{6.9}$, $TlBa_2CaCu_2O_7$, and $Tl_2Ba_2CaCu_2O_8$ single crystals are investigated by Raman spectroscopy. The temperature dependence of the O phonon frequency and linewidth is fit using the results of a perturbation calculation of Raman scattering from anharmonic vibrations with very good results, provided both third- and fourth-order terms in the phonon self-energy are included. Temperature-dependent asymmetric Fano line shapes of the apex O modes, which are observed especially well in $TlBa_2CaCu_2O_7$, suggest significant coupling of these modes to the background continuum. From the temperature dependence of the background intensity we deduce that the Raman scattering continuum in the region 100–1000 cm^{-1} contains significant two-particle scattering. The zz polarization of the observed scattering suggests the background is due to two-phonon rather than two-magnon scattering. The Fano line shape and the temperature dependence of the asymmetry can then be attributed to anharmonic interactions.

I. INTRODUCTION

Anharmonicity of high-frequency O vibrations in high-T_c oxides has attracted considerable attention because of a possible connection with the mechanism for superconductivity.[1] Anharmonic O vibration potentials resulting from O valence fluctuations have been recently shown to be responsible for the lattice instability in La_2CuO_4.[2] The behavior of the anharmonic modes in high-T_c oxides are thus of interest both from the point of view of the superconductivity and lattice stability of the cuprate superconductors.

It has been found in high-temperature Raman scattering experiments[3–5] that particularly apex O vibrational modes show fairly strong temperature dependence of vibration frequencies and linewidths while other modes involving planar O ions show a much smaller shift or broadening in the same temperature range.

In this paper we analyze the temperature dependence of the frequencies and linewidths of selected O phonons in terms of a model calculation for the Raman scattering including higher-order anharmonic potentials in the Hamiltonian. We compare the predictions of the model with experimental Raman data on single crystals in three high-T_c materials: $YBa_2Cu_3O_{6.9}$ (YBCO), $TlBa_2CaCu_2O_7$ (Tl 1:2:1:2), and $Tl_2Ba_2CaCu_2O_8$ (Tl 2:2:1:2) in the temperature range 5–1000 K. We also analyze the line shapes in Tl 1:2:1:2 and suggest an origin for the phonon line asymmetry related to the observed anharmonicity. We also analyze the temperature dependence of the background "continuum" and suggest that it contains a very significant contribution from two-particle scattering in the region 100–1000 cm^{-1}.

In strongly absorbing materials such as high-T_c cuprates, the Raman scattering process can be viewed as the absorption of a photon with energy $\hbar\omega_i$ and the emission of a scattered photon of energy $\hbar\omega_s$ simultaneously with the creation of a phonon of energy $\hbar\omega_0$. The main contribution to the phonon lifetime is usually the decay of the phonon into two or more phonons via the anharmonic interaction. The temperature dependence of the phonon frequency and linewidth reflects the temperature dependence of the phonon's self-energy, $P(\mathbf{q},\omega)$. At $\mathbf{q}=\mathbf{0}$,[6]

$$\lim_{\epsilon\to 0} P(\omega+i\epsilon) = -\frac{\hbar}{k_B T}[\Delta(\omega) - i\Gamma(\omega)], \tag{1}$$

where ω is the phonon frequency and T is the temperature.

Temperature-dependent frequency softening and line broadening have been previously investigated in silicon by Balkanski *et al.*,[7] and theoretical calculations using perturbation theory and an anharmonic potential were in very good agreement with Raman measurements. We apply the results of their calculation and fit the results to experimental data on the high-T_c oxides. Both third- and fourth-order anharmonicities have been included in the model, and fitting the results to the experimental data gives us the possibility of extracting information regarding also the higher-order anharmonicity parameters of the O modes in high-T_c oxides.

II. EXPERIMENTAL RESULTS AND ANALYSIS

A. Frequencies

The frequencies of the apex O vibrations as a function of temperature are shown in Fig. 1 for the three

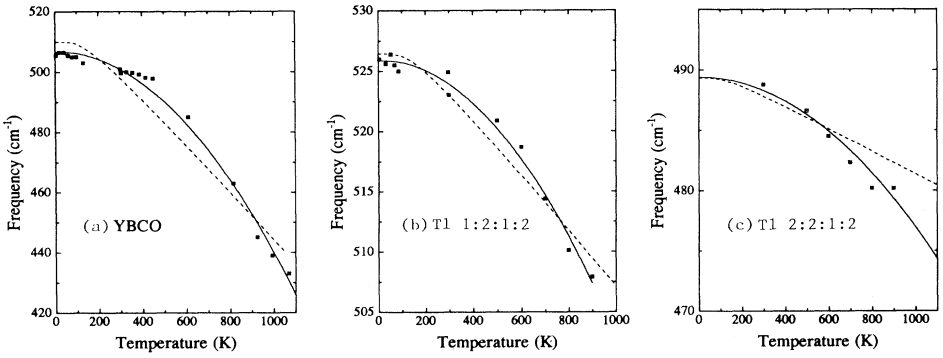

FIG. 1. Frequency of the z axis apex O vibration in (a) $YBa_2Cu_3O_{6.9}$, (b) $TlBa_2CaCu_2O_7$, and (c) $Tl_2Ba_2CaCu_2O_8$ as a function of temperature. The solid line is a fit to the data using Eq. (2). The dashed lines show a fit using only the contribution from Δ_1. The linewidth of $TlBa_2CaCu_2O_7$ is determined from a fit to a Fano line shape, and the frequency shift is given by V^2R (see Sec. II B).

different materials under investigation here. The actual Raman spectra at different temperatures have already been published,[4,8] and the details of the experiments, especially relating to the O out-diffusion problem, can be found there. Importantly, $YBa_2Cu_3O_{6.9}$ was heated in an O atmosphere, which ensures that the O level is kept in equilibrium. Also crucially, the spectra were carefuly compared before and after heating to make sure that no irreversible changes took place during the heating cycle. The present paper presents the results of a careful fit of the linewidths, line shapes, and frequencies over an extended range of temperatures.

We see a universal frequency softening of the apex O mode with temperatures in the range 5–1000 K which is largest ($\sim$ 65 cm^{-1}) in $YBa_2Cu_3O_{6.9}$, and smallest ($\sim$ 20 cm^{-1}) in $TlBa_2CaCu_2O_7$ and $\sim$ 15 cm^{-1} in $Tl_2Ba_2CaCu_2O_8$. The frequencies were determined by fitting a Lorentz function to the spectra. Some error in the determination of the Raman frequency is introduced because the wings of the lines cannot be always accurately fit. The worst is the case of Tl 2:2:1:2, with considerably better fits in YBCO and Tl 1:2:1:2. For Tl-1:2:1:2 we have also used a Fano function to fit the lines, which we found to describe the line shape much better. The line shapes will be discussed in more detail later. The frequency shifts of the *other* modes observed in Raman scattering are negligible over the same 1000 K temperature range,[3,8] and so they are omitted from further discussion in this paper.[9]

Following Balkanski,[7] the temperature-dependence of the $\mathbf{q} = \mathbf{0}$ Raman phonon frequency is given by

$$\omega = \omega_0 - A\Delta_1(T) - B\Delta_2(T), \tag{2}$$

where

$$\Delta_1(T) = 1 + \frac{2}{e^x - 1} \tag{3}$$

and

$$\Delta_2(T) = 1 + \frac{3}{e^y - 1} + \frac{3}{(e^y - 1)^2}, \tag{4}$$

where ω_0 is the $T = 0$ phonon frequency, and $x = \frac{\hbar\omega_0}{2kT}$ and $y = \frac{\hbar\omega_0}{3kT}$. The temperature-dependent terms in (2) represent the real part of the proper phonon self-energy (1). The constants A and B determine the cubic and quartic contributions, Δ_1 and Δ_2 respectively. The temperature dependence in the self-energy arises solely due to Bose-Einstein factors, while the matrix elements for the transitions are assumed to be temperature independent.[7] The final states into which the anharmonic phonon decays are not identified explicitly. Instead, it is assumed that the anharmonic phonon of energy $\hbar\omega_0$ decays into two other phonons, each carrying off energy $\hbar\omega_0/2$ in the cubic case, and three phonons of energy $\hbar\omega_0/3$ in the quartic case. Because of the large number of phonons in the oxides, it is not difficult to find modes at the right frequencies and wave vectors to satisfy energy conservation.

The results of fitting (2) to the high-temperature Raman data is shown superimposed in Fig. 1 and the anharmonic coefficients A and B obtained are given in Table I. In the high-temperature limit, ($k_BT \gg \hbar\omega_0$),

TABLE I. Anharmonic coefficients obtained by fitting the line frequencies and linewidths (FWHM) of the apex O modes as a function of temperature.

	ω_0 (cm^{-1})	A (cm^{-1})	B (cm^{-1})	Γ_0 (cm^{-1})	C (cm^{-1})	D (cm^{-1})
$YBa_2Cu_3O_{6.9}$	507 ± 1	<0.1 ± 0.1	1.3 ± 0.3	10 ± 2	14 ± 2	< 0.1 ± 0.1
$TlBa_2CaCu_2O_7$	526 ± 1	< 0.1 ± 0.1	0.5 ± 0.1	6.5 ± 1	8 ± 1	0.3 ± 0.3
$Tl_2Ba_2CaCu_2O_8$	489 ± 1	0.4 ± 0.2	0.23 ± 0.05	26 ± 5	3.8 ± 2	0.9 ± 0.4

Δ_1 is linearly proportional to the absolute temperature, while Δ_2 includes both a linear and quadratic temperature dependence. From Fig. 1 we see that the frequency shifts have a significant T^2 dependence, implying a large contribution from higher-order processes contributing to Δ_2. For reference, fits using only two-phonon decay (cubic terms) are also shown in Fig. 1. They show that a satisfactory fit cannot be obtained using only cubic anharmonicity. This observation is in apparent qualitative agreement with x-ray appearance near-edge structure (XANES) data, where Conradson *et al.*[1] have used a predominantly quartic potential to fit their data.

B. Line shapes

As has already been remarked by Gasparov *et al.*,[10] the apex O vibrations are asymmetric and show a steep edge on the high-energy side of the phonon lines. This is not usually noticeable in $YBa_2Cu_3O_7$ because an additional — possibly impurity — induced infrared-active (IR) mode at 580 cm^{-1} fills the wing of the apex O line on the high-frequency side. In $Tl_2Ba_2CaCu_2O_8$, there are three modes above 400 cm^{-1}, and their wings have significant overlap, again making a quantitative analysis of the lineshape difficult. Fortunately, no other modes are present on either side of the apex O line in $TlBa_2CaCu_2O_7$ and the asymmetry of the apex O mode can be clearly seen. (The 460 cm^{-1} mode is clearly visible only in the low-temperature spectra.) The departure from the Lorentz profile is quite significant, which is especially clearly seen in Fig. 2. Although Gasparov *et al.*[10] have suggested that possibly forbidden IR modes appearing on the low-energy side could cause an apparent asymmetry, we find that a fit using one or even two additional Lorentz lines gives rise to unphysically large 80–100 cm^{-1} linewidths for these additional modes.

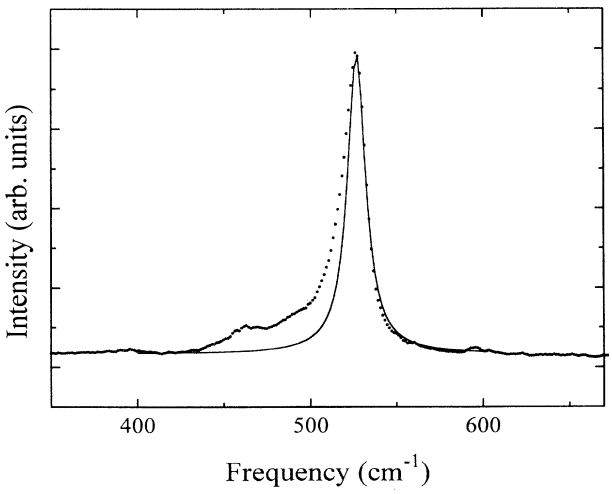

FIG. 2. A Lorentz fit to the 5 K Raman spectrum of the apex O line in $TlBa_2CaCu_2O_7$ clearly showing an asymmetry in the line shape. Note that although additional oscillators can be added in the model to fit the low-frequency wing, this results in unphysically large linewidths (see text).

An asymmetric phonon line shape in cuprate superconductors is usually attributed to the interference between the phonon and a background continuum of states and is often described using the Fano formalism.[11] The Fano line shape for a phonon coupled to a background "continuum" is given by

$$l(\epsilon) \propto \frac{(q+\epsilon)^2}{1+\epsilon^2}, \tag{5}$$

where

$$\epsilon = \frac{\omega - \omega_0 - V^2 R}{\pi V^2 \rho}, \tag{6}$$

and V is the interaction strength between the phonon and the continuum. The density of states in the continuum ρ and the bare phonon energy ω_0 are held constant in the fit, while V, R, and q are allowed to vary. The fit to Eq. (5) for the spectra of the apex O in $TlBa_2CaCu_2O_7$ at various temperatures is shown in Fig. 3 and can be seen to describe the experimental line shape very well. We attribute the departure from the fitted line shape due to additional broadening from disorder. The quantities that can be directly interpreted are V^2R and $2\pi V^2\rho$, and are the line*shift* and line*width*, respectively. The two quantities are plotted in Figs. 1 and 4, respectively. The Fano analysis is quite general and says nothing about the origin for the states involved, nor about the interaction responsible for the interference. Most often it is

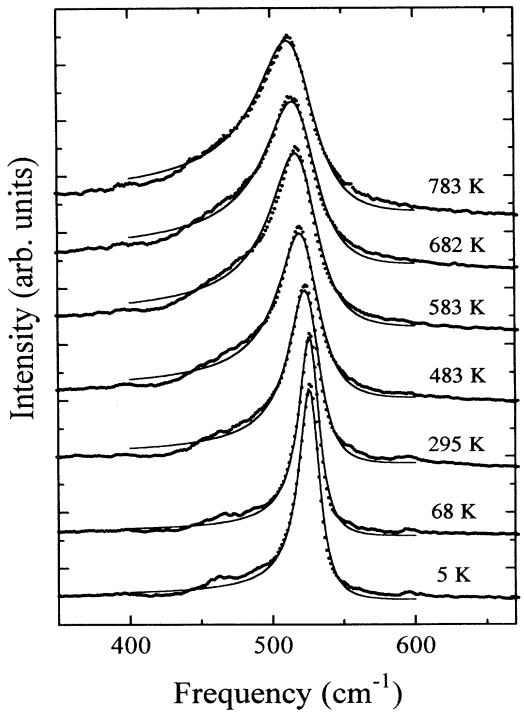

FIG. 3. Apex O Raman spectra of $TlBa_2CaCu_2O_7$ at different temperatures. A single Fano function (5) can be used to fit the line shape very well. No additional parameters were used in the fits except a constant background. The intensity of the 460 cm^{-1} mode is very small. At higher temperatures it broadens significantly and is no longer identifiable, but in all cases it can be ignored in the fitting.

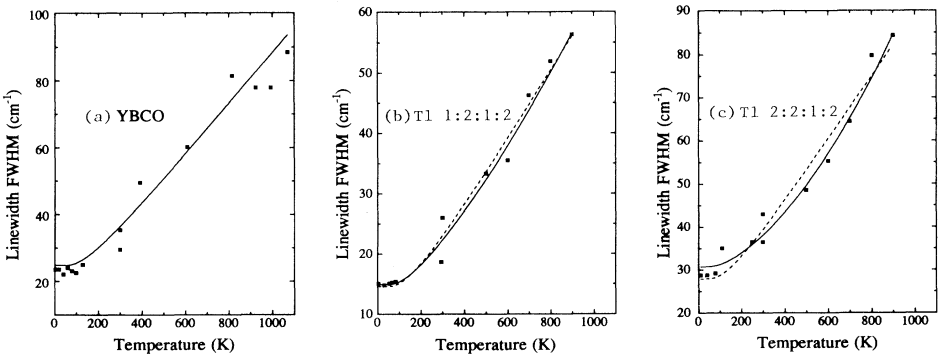

FIG. 4. Linewidth (FWHM) of the apex O vibration in (a) $YBa_2Cu_3O_{6.9}$, (b) $TlBa_2CaCu_2O_7$, and (c) $Tl_2Ba_2CaCu_2O_8$ as a function of temperature. The solid line is a fit to the data using Eq. (7). The five linewidth data points for T<300 K for Tl 2:2:1:2 were taken from Ref. 10 . The linewidth in (b) is given by $2\pi V^2\rho$. The dashed lines show a fit using only the Δ_1 term.

a phonon and an electronic continuum which interfere through electron-phonon coupling. However, Rousseau and Porto have shown that an asymmetric line shape can also result from the interference between a one-phonon state and a two-phonon background via the anharmonic interaction. This was demonstrated on a related perovskite, $BaTiO_3$.[12] Since the anhamonic interaction is reasonably large for the apex O modes in the superconducting oxides, we can expect here also that the asymmetry of the modes could be due to the interaction between the one-phonon states and the two-phonon (or even three-phonon) background. Why we suggest this, rather than the interaction between the phonon and an electronic background, will be apparent later.

There are a number of observations which support this hypothesis. In Fig. 3 we see that the asymmetry of the line shape is highly temperature dependent. This implies that also the *coupling* of the phonon to the background is also temperature dependent. Such a temperature dependence is indeed expected in the case of anharmonic coupling,[13] but *not* usually in the case of straightforward electron-phonon coupling. We also note that the line shape cannot be fit using a temperature-*dependent* but symmetric part, plus a temperature-*independent* asymmetric part to the line shape. This would be concievably the case if an anharmonic phonon would also be coupled to an electronic background, i.e., the origin of the temperature dependence and Fano line shape was different. To what extent there is also mixing with an electronic background could be determined by comparison of the magnitude of the Fano interference effects in different scattering geometries. The different selection rules for the interference between the phonon and an electronic continuum or a two-phonon or three-phonon background could then be used to distinguish between the two contributions — assuming that we have precise knowledge of the scattering tensor components in both cases.

C. Linewidths

The linewidths (FWHM) of the apex O modes as a function of temperature are shown in Fig. 4. The linewidths were determined by (a) fitting a Lorentzian function in the case of YBCO and Tl 2:2:1:2 where the wings are obscured by other phonons and (b) by fitting a Fano function (5) to the Tl 1:2:1:2 spectra, where the linewidth is given by $2\pi V^2\rho$. The linewidth temperature-broadening in the temperature range 5 – 1000 K in the three materials is approximately 65 cm^{-1} in $YBa_2Cu_3O_{6.9}$, 50 cm^{-1} in $TlBa_2CaCu_2O_7$, and 60 cm^{-1} in $Tl_2Ba_2CaCu_2O_8$. Assuming that anharmonic decay limits the phonon lifetime, the temperature-dependence of the phonon linewidth Γ_a is given by

$$\Gamma_a = C\Delta_1(T) + D\Delta_2(T), \tag{7}$$

where C and D are the anharmonicity parameters, again corresponding to the three- and four-phonon contributions to the imaginary part of the self-energy (1).

Fits of Eq. (7) to the experimental data are shown superimposed on the data in Fig. 4. The fitted values of the parameters are listed in Table I for the three different materials. We have found that the we could not obtain a fit of (7) to the data, unless we assumed that the linewidth was not entirely due to anharmonic decay. A very good fit can be obtained, however, if we include in the fit an additional (perhaps disorder-induced) linewidth Γ_0, such that the full linewidth $\Gamma = \Gamma_a + \Gamma_0$ and Γ_0 is for the moment assumed to be temperature independent. (The values of Γ_0 are also given in Table I.) The origin of the additional broadening is most likely disorder in the material, although additional processes limiting the lifetime of the apex O phonons cannot be ruled out, and should be studied further. Taking the data of the linewidths of the apical O mode in $TlBa_2CaCu_2O_8$ as the most reliable (for reasons already mentioned in the previous section) we observe in Fig. 4 a predominantly linear temperature dependence above 200 K, with only a small quadratic term. The fit to the phonon linewidth in $Tl_2Ba_2CaCu_2O_8$ is also predominantly linear in T, while the data for YBCO are rather scattered, so there we cannot conclude about higher-order contributions.

The intrinsic linewidths Γ_a deduced from the fits suggest low-temperature phonon lifetimes $\tau = 2/\Gamma_a$ for the

apex O modes around 0.7 ± 0.5 ps for $YBa_2Cu_3O_{6.9}$, 1.5 ± 1 ps for $TlBa_2CaCu_2O_7$ and 2.0 ± 1 ps in $Tl_2Ba_2CaCu_2O_8$. These values are significantly shorter than the 7.5 ps found for the LO mode in Si (Ref. 7).

D. Two-particle Raman *continuum*

Since the first observations of a broad continuum in the Raman spectra of superconducting cuprates,[14] the issue has received a large amount of experimental[15] and theoretical[16] attention. The continuum is seen in virtually all scattering geometries, including zz scattering, which is of special interest in the present work, as we are able to analyze the continuum scattering at higher temperatures than is usually done. So far to our knowledge the possibility of the presence of a multiphonon background in the Raman spectra has not been seriously considered, and since we have suggested in the previous section that the Fano line shapes imply the existence of such a background, we analyze now this possibility further. Although all three materials investigated here show a temperature-dependent continuum in zz scattering geometry, we will concentrate the analysis on Tl 1:2:1:2, where the spectrum contains the fewest one-phonon lines, making the analysis easier. In Fig. 5 we have plotted a number of Tl 1:2:1:2 spectra at different temperatures superimposed on each other. For temperatures below 300 K, the background intensity does not change significantly and its ω dependence is fairly flat. Above room temperature, the background intensity starts to increase dramatically, especially below 500 cm^{-1}. The background appears to fall off at frequencies above 600 cm^{-1}, which is expected for two-phonon scattering, where the shape approximately reflects the total density of two-phonon states $N(2\omega)$.

If we assume that the background scattering consists of single-paticle and two-particle scattering (of unspecified origin), we can write the Stokes differential Raman scattering cross section as a sum of the contributions from first-order and second-order scattering processes:

$$\frac{d^2\sigma}{d\Omega\, d\omega} = \left(\frac{d^2\sigma}{d\Omega\, d\omega}\right)_1 + \left(\frac{d^2\sigma}{d\Omega d\omega}\right)_2^+ + \left(\frac{d^2\sigma}{d\Omega\, d\omega}\right)_2^-, \quad (8)$$

where the first term is the one-particle scattering cross section, while the last two terms on the right are the cross sections for the sum-mixing and difference-mixing two-particle scattering processes. The thermal factors for the Stokes scattering can be written explicitly:

$$\begin{aligned}\frac{d^2\sigma}{d\Omega\, d\omega} &= S_1(\omega)(n+1) \\ &\quad + \sum_{i,j}\{S_2^+(\omega)(n_i+1)(n_j+1) \\ &\quad + S_2^-(\omega)n_i(n_j+1)\}, \end{aligned} \quad (9)$$

where n_i is the Bose factor, $1/[\exp(\hbar\omega_i/k_BT) - 1]$, and the sum in the second-order scattering is over all phonons i, j. $S_1(\omega)$ and $S_2^{\pm}(\omega)$ are the temperature-independent parts of the one- and two-particle cross sections. From (9) we see that the contributions from one- and two-particle scattering processes can be separated out experimentally from the temperature dependence of the background intensity over a sufficiently large temperature range. We have chosen five different points (at 100, 200, 300, 370, and 700 cm^{-1}) in the continuum and plotted their scattering intensity against temperature in Fig. 6. For only first-order scattering (for example, from a solely electronic continuum), we expect $\frac{d^2\sigma}{d\Omega\, d\omega} \propto (n+1)$ and at higher temperatures $\frac{d^2\sigma}{d\Omega\, d\omega} \propto T$. In the data, however, we observe a significant quadratic component in the T

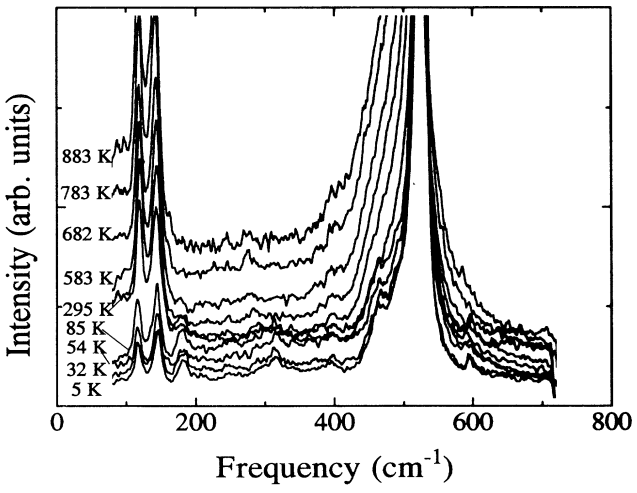

FIG. 5. A sequence of spectra of Tl 1:2:1:2 at different temperatures. The baseline is the same for all spectra and no thermal factors have been divided out. The spectra have been normalized in intensity to the apex O phonon, which is assumed to have an $(n+1)$ temperature dependence.

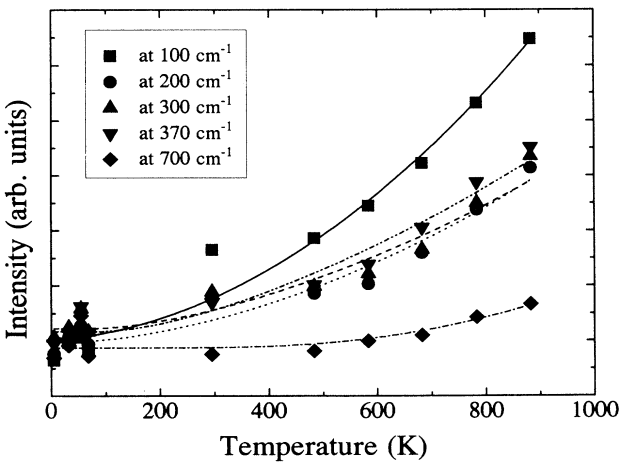

FIG. 6. The background intensity of Tl 1:2:1:2 at five different frequencies as a function of temperature. The lines are fits using linear and quadratic temperature-dependent terms derived from Eq. (9). The quadratic terms arise from two-particle scattering processes.

dependence above 300 K, indicative of second-order n^2 terms in the cross section (9), which can only arise from higher-order scattering.

The particles involved in the scattering could in principle be magnons, phonons, etc. Two-magnon scattering, which is present in the insulating, antiferromagnetic (AF) species of the material, could concievably be present due to short-range spin correlations remaining in the superconducting phase. Two-magnon scattering in the case of two-dimensional AF ordering has very clear selection rules, however, which prohibit its observation in zz scattering geometry.[17] Since the present spectra were taken in zz scattering, this appears to exclude simple two-magnon scattering as the origin of *these* spectra. However, in the presence of significant spin-lattice coupling and/or significant buckling of the CuO_2 planes in the doped materials the selection rules could be somewhat relaxed to allow some very weak, but nonzero two-particle zz scattering to be observed. Alternatively, since the cutoff at twice the maximum phonon frequency and peak of the spectrum at 600 cm^{-1} or so very much resembles the shape expected for the two-phonon density of states (2PDOS), we suggest instead that we are most likely dealing with two-phonon scattering which is nonzero in the zz scattering geometry. The relatively featureless background is consistent with the large number of strongly dispersed phonons in these materials. Nevertheless, there is some structure in the background, and a comparison between 2PDOS and the spectral shape could possibly lead to identification of the unassigned features in the Raman spectra. The temperature dependence of the background would thus independently confirm our original supposition of the presence of sigificant two-phonon scattering intensity in the continuum background at frequencies in the region 100–1000 cm^{-1}.

III. DISCUSSION

Given that the high-temperature behavior of the apex O ions can be described using a phenomenological theory of vibrational anharmonicity, the questions of the microsopic origin of the anharmonicity and its consequences still remain. A serious problem with interpreting frequency softening and temperature-dependent linewidths of O modes in high-T_c materials arises from the O motion and disorder at higher temperatures. Because the temperature softening and broadening is the same in $YBa_2Cu_3O_{6.9}$ and $YBa_2Cu_3O_{6.2}$, we can probably safely deduce that the disorder in the O(1) and O(5) sites is not *directly* causing the effects we observe. O ions are known to be quite mobile in $YBa_2Cu_3O_{7-\delta}$, but are virtually immobile in the thallium compounds. There does not appear to be any connection between the temperature dependence of the apical O phonon linewidths and O mobility in the material. In order to make a possible connection between the O hopping or transport between interstitial sites and the anharmonicity of the O vibrations in the vicinity of such sites we need a microscopic theory which is beyond the scope of this paper.

A perhaps surprising result of the analysis of the temperature dependence of apex O vibration frequencies and linewidths is that whereas the frequency shifts have a primarily quadratic T dependence, the linewidths show essentially linear behavior in the same temperature range; i.e., whereas in the real part of the self-energy, the Δ_2 term is dominant, in the imaginary part the Δ_1 term appears larger. The reason for this could be found if we consider the vertex diagrams that are used in the calculation of the self-energy. In the real part, $\Re[P(\mathbf{q},\omega)]$ some higher-order diagrams are included [shown in Fig. 1(d) of Ref. 7] which are not present in the imaginary part $\Im[P(\mathbf{q},\omega)]$. These diagrams could have a major contribution to Δ_2, judging by the large coefficient B in Table I. Additionally, similar diagrams which contribute to Δ_2 and not Δ_1 may also occur due to defect scattering,[13] local modes, or other similar processes. The defect contribution appears to be particularly large judging by the frequency shift in YBCO, which is more than twice the size of that in the other two materials studied here. Conversely, disorder does not appear to affect the imaginary part of the self-energy as much, judging by the fact that the linewidth changes with temperature in YBCO, Tl 1:2:1:2, and Tl 2:2:1:2 are of approximately the same magnitude.

Unfortunately, we cannot determine the origin of the different higher order vertex contributions to $\Re[P(\mathbf{q},\omega)]$ from the temperature-dependence data presented here, since they all give rise to either a linear or quadratic T dependence at high T. The effect of defects on $P(\mathbf{q},\omega)$ could be studied if samples with different concentrations of (temperature-independent, but coupled) defects could be made.

The perturbation calculation used to fit the data in the present paper relies on anharmonic corrections to the harmonic Hamiltonian. We therefore cannot make direct comparisons with the results of the extended x-ray absorption fine-structure (EXAFS) data,[1] where the authors have used a double well or a combined set of two harmonic potentials in describing their data. Nevertheless, a large quartic contribution to the anharmonic hamiltonian agrees qualitatively with their findings. It would be interesting to calculate whether the observed T and T^2 dependences at high temperatures in the Raman frequency and linewidth can also be predicted by their model. Another possibility for describing the anharmonic effects of the O modes would be to use the shell model[18] of the electron-phonon interaction which includes both short-range and long-range interactions. The results of such first-principles calculations may be preferable to the perturbation treatment for the relatively large quartic anharmonicity found in the Raman data, especially if it can be extended to a nonzero wave vector.

Given that we have dealt with the anharmonicity as a perturbation, this suggests the effects to be too small to be responsible for the high critical temperatures in the cuprates. We should stress however that the present Raman scattering experiments are looking strictly at the anharmonicity of vibrations at $q \approx 0$. Regarding superconductivity, there may be much larger effects at a nonzero wave vector, which the present experiments do not probe, but which are known to be present from neutron measurements, for example,[19] and so no definite conclusions

on the relevance to superconductivity can be reached on the basis of these data alone.

Finally, we should remark that in the analysis of the background it has been sometimes useful to present spectra with a thermal factor $(n + 1)$ divided out. Following the discussion of the previous section it appears that dividing the entire spectrum by $(n + 1)$ could be sometimes misleading, since the background which also contains two-particle processes will have prefactors of $(n_1 + 1)(n_2 + 1)$ or $n_1(n_2 + 1)$ rather than just $(n + 1)$. The resulting spectral shapes could be rather distorted, especially at low frequencies, leading to misinterpretation of the Raman scattering continuum.

IV. CONCLUSION

In conclusion, O disorder in itself cannot account for the temperature dependences of apex O vibrations which we observe in Raman scattering experiments. The best evidence for this is the fact that $YBa_2Cu_3O_{7-\delta}$, with $\delta \sim 1$ and $\delta \sim 0$, behave in virtually the same way.[3] The temperature dependence of the self-energy in YBCO and Tl compounds is very similar, even though O is very mobile in YBCO but much less so in the Tl compounds up to quite high temperatures.

Instead, the very good agreement between the experimental temperature dependence of the $q \approx 0$ apex O vibration frequencies and linewidths with theoretical calculations of anharmonic phonon self-energy suggest inherent anharmonicity in these materials. Although not as large as in some prototype anharmonic crystals, larger anharmonicities may be observable at a nonzero q vector, with special relevance to phonon-mediated superconducitivity. We emphasize again that other modes in the Raman spectra do not show such strong temperature dependences. The anharmonic effects in the imaginary part of the self-energy are found to be comparable in all three materials investigated. The largest softening in the frequency found in $YBa_2Cu_3O_{6.9}$ is suggested to be due to the large contribution from defect scattering vertices in the real part of the self-energy.

Both the strong temperature dependence of the asymmetric line shapes and the quadratic temperature dependence of the background scattering intensity suggest that the background is in large part due to second-order scattering. Two-magnon scattering being excluded by the zz polarization of the observed scattering, two-phonon scattering is the most likely origin of the scattering. The asymmetric line shapes are then believed to arise because of anharmonic coupling of phonons to the two-phonon background.

ACKNOWLEDGMENTS

We wish to acknowledge valuable comments from I. Batistić and I. Sega. We also wish to thank G. Collin for YBCO single crystals which were used for part of this work. This work has been supported in part by CEC Grant No. CI1 0568-C and the DOE Grant No. JF-020 as well as the Ministry for Science and Technology of Slovenia.

[1] J. Mustre de Leon *et al.*, Phys. Rev. Lett. **65**, 1675 (1990); also S.D.Conradson, I.D.Raistrick, and A.R.Bishop, Science **248**, 1394 (1990).

[2] A. Bussmann-Holder *et al.*, Phys. Rev. Lett. **67**, 512 (1991).

[3] D. Mihailovic and C.M. Foster, Solid State Commun. **74**, 753 (1989); I. Poberaj and D. Mihailovic, Phys. Rev. B **42**, 393 (1990).

[4] D. Mihailovic, K.F. McCarty, and D.S. Ginley, Ferroelectrics **130**, 107 (1992); also L.V. Gasparov, V.D. Kulakovskii, V.B. Timofeev and V.Ya. Sherman, Zh. Eksp. Teor. Fiz. **100**, 1681 (1991) [Sov. Phys. JETP **73**, 929 (1991)].

[5] I. Ohana *et al.*, Phys. Rev. B **40**, 2562 (1989).

[6] I.P. Ipatova, A.A. Maradudin, and R.F. Wallis, Phys. Rev. **155**, 882 (1967); R.F. Wallis, I.P. Ipatova, and A.A. Maradudin, Fiz. Tverd. Tela Leningrad **8**, 1064 (1966) [Sov. Phys. Solid State **8**, 850 (1966)].

[7] M. Balkanski, R.F. Wallis, and E. Haro, Phys. Rev. B **28**, 1928 (1983).

[8] K.F. McCarty *et al.*, Phys. Rev. B **38**, 2914 (1988).

[9] An exception is the O(3) z axis vibration at 602 cm^{-1} vibration in $Tl_2Ba_2CaCu_2O_8$, which shows a 15 cm^{-1} softening over 1000 K and a much smaller (20 cm^{-1}) line broadenening. This suggests qualitatively different behavior compared with the apex modes and which warrants further investigation. The data on the frequency shifts of all the modes and the actual spectra are shown in Ref. 4.

[10] L.V. Gasparov *et al.*, Physica C **160**, 147 (1989).

[11] U. Fano, Phys. Rev. **124**, 1866 (1961); U. Fano and J.W. Cooper, *ibid.* **137**, A1364 (1965).

[12] D.L. Rousseau and S.P.S. Porto, Phys. Rev. Lett. **20**, 1354 (1968).

[13] R.A. Cowley, in *The Raman Effect*, edited by A. Anderson (Marcel Dekker, New York, 1971), Vol. 1, pp. 95–151.

[14] D. Mihailovic *et al.* Phys. Rev. B **36**, 3997 (1987); S.L. Cooper *et al.*, *ibid.* **37**, 5920 (1988).

[15] D. Reznik *et al.*, Physica C **185-189**, 1029 (1991), and references therein; also D. Reznik *et al.* (unpublished).

[16] C.M. Varma *et al.*, Phys. Rev. Lett. **63**, 1996 (1989); A. Virtosztek and J. Ruvalds, Phys. Rev. B **45**, 347 (1992); P.W. Anderson, Physica C **185-189**, 11 (1991).

[17] J.B. Parkinson, J. Phys. C **2**, 2012 (1969); K.B. Lyons, P.A. Fleury, L.F. Schneemeyer, and J.V. Waszczak, Phys. Rev. Lett. **60**, 732 (1988).

[18] A. Bussmann-Holder and A.R. Bishop, Phys. Rev. B **44**, 2853 (1991).

[19] W. Reichardt, N. Pyka, L. Pintschovius, B. Hennion, and G. Collin, Physica C **162-164**, 464 (1989); also H. Reitschel, L. Pinschovius, and W. Reichardt, Physica C **162-164**, 1705 (1989); L. Pintschovius *et al.*, *ibid.* **185-189**, 156 (1991).